



Fabrication of cyanine dye thin films grown by a layer-by-layer method

Nagauchi, Junpei
Kojima, Osamu
Kita, Takashi
Shim, YongGu

(Citation)

Materials Research Express, 2(7):076402-076402

(Issue Date)

2015-07

(Resource Type)

journal article

(Version)

Accepted Manuscript

(Rights)

© 2015 IOP Publishing. This is an author-created, un-copyedited version of an article accepted for publication/published in Materials Research Express. IOP Publishing Ltd is not responsible for any errors or omissions in this version of the manuscript or any version derived from it. The Version of Record is available online at...

(URL)

<https://hdl.handle.net/20.500.14094/90003776>



Fabrication of cyanine dye thin films grown by a layer-by-layer method

Junpei Nagauchi¹, Osamu Kojima¹, Takashi kita¹ and YongGu Shim²

¹Department of Electrical and Electronic Engineering, Graduate School of Engineering, Kobe University, 1-1 Rokkodai, Nada, Kobe 657-8501, Japan

²Department of Physics and Electronics, Graduate School of Engineering, Osaka Prefecture University, 1-1 Gakuen-cho, Naka-ku, Sakai, Osaka 599-8531, Japan

E-mail: kojima@phoenix.kobe-u.ac.jp

Abstract. We report the optical properties of the cyanine dye molecule thin film fabricated by a layer-by-layer method. While the absorbance and the film thickness increase with the dipping time, the use of a multilayer structure enables fabrication of the thin film without the creation of the molecule bundle that suppresses light scattering and the large absorbance obtained for the shorter dipping time. Exciton dynamics are studied by using a pump-probe technique; the signal shows two decay components in the multilayer sample that originates from the fast intramolecular relaxation and from the slow exciton relaxation. The temporal profiles show at the high signal-to-noise ratio. These results indicate that the thin film without the creation of the molecule bundle fabricated by the layer-by-layer method can be used for ultrafast all-optical switches.

PACS numbers: 78.40.Me, 78.47.D-, 78.66.Qn

1. Introduction

Organic molecules have attracted considerable attention for various optoelectronic devices including light emitting diodes [1-4], photovoltaic cells [5-7], and field-effect transistors [8-13]. In particular, the optical nonlinearities of organic molecules have been intensely investigated, because a high optical nonlinearity is essential for the realization of all-optical switches in a next-generation high-speed optical communication network. For the typical molecules, the intramolecular relaxation rate approaches 1 ps^{-1} [14-20], implying that an ultrafast nonlinear optical response may be possible; this is highly attractive for applications. For instance, the cyanine dye molecules are one of the candidate ultrafast optical materials because of their optical characteristics, including the tunability of the absorption wavelength and the ultrafast response [14-16, 20, 21]. While the basic device performance is controlled by the optical properties, to achieve a high signal-to-noise ratio, fabricating the thin film with a flat surface is a key issue.

To fabricate the thin film, we have focused on a layer-by-layer (LBL) method [22]. The LBL method, which uses electrostatic attraction [23-25], can be expected to create a flat surface that will increase the signal-to-noise ratio in the optical signal as well as in the pump-probe signal. However, in our previous report, although the dynamics were evaluated from the photoluminescence measurements with the time resolution of 40 ps, it was difficult to obtain a signal with a high signal-to-noise ratio in the thick samples. To solve this problem, we focused on the multilayer structure. Therefore, in this study, we report the fabrication of the multilayer structure cyanine dye thin films by the LBL method and the optical characteristics of these films. The optical characteristics were evaluated from the absorption spectrum and the transmittance change signal. The large absorbance and the surface without the creation of the molecule bundle were realized by systematically changing the dipping time. Because of the surface, the relaxation dynamics were clearly observed. The optical characteristics are discussed from the viewpoint of the effective thin film fabrication.

2. Experiment

We used a commercial cyanine dye molecule 2-[2-[2-Chloro-3-[2-(1,3-dihydro-1,1,3-trimethyl-2H-benz[e]indol-2-ylidene)ethylidene]-1-cyclohexen-1-yl]ethenyl]-1,1,3-trimethyl-1H-benz[e]indolium-4-methylbenzenesulfonate (PSA1411) purchased from Tosco Co., Ltd. without further purification. The chemical structure is shown in Fig. 1. The glass substrates were cleaned by immersion in a fresh piranha solution (2/5 (v/v) mixture of 30% H_2O_2 and 98% H_2SO_4) for 60 min. The substrates were carefully rinsed with water and used immediately after cleaning. The LBL assembly was performed by sequentially dipping the substrates in the aqueous solution. The PSA1411 is positively charged in the aqueous solution and adsorbed to the substrate for the different dipping times that varied from 10 s to 1 h. The spacer layer comprises the positively charged poly(diallyldimethylammonium chloride) (PDDA) and negatively charged poly

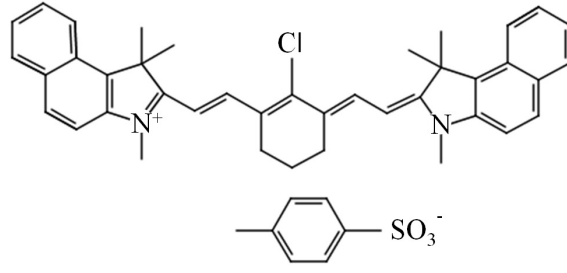


Figure 1. Chemical structure of PSA1411.

(acrylic acid) (PAA). In the beginning of the sample preparation, the adhesion layers of (PAA/PDDA)₃, where the subscript indicates the number of the pairs of PAA and PDDA, were deposited to enhance the binding of the dye molecule layer to the substrate. Finally, we covered the samples with poly(vinyl alcohol) (PVA) by spin coating to reduce the photodegradation. The PVA has an excellent gas-barrier property [26, 27].

The absorption spectrum was measured by using a 100-W halogen lamp and a spectrometer with a resolution of 6 nm. Spectroscopic ellipsometry (HORIBA Jobin-Yvon, UVISSEL-TK9017TK) was used to accurately determine the layer thickness of the polymers and PSA1411. The measurement was performed by the spectroscopic phase modulated ellipsometer in the spectral range from 0.76 to 6.0 eV. The transient response was measured by a time-resolved transmission-type pump-probe technique. The light source used was a mode-locked Ti:sapphire pulse laser with a pulse width of approximately 100 fs and a repetition rate of 80 MHz. The pump and probe powers were kept at 63.7 and 3.18 nJ/cm², respectively. The pump energy was tuned to 1.55 eV. The pump and probe beams were orthogonally polarized each other, resulting in the elimination of the pump-beam contribution to the probe beam. The pump beam was modulated at 2 kHz by an optical chopper. The intensity of the probe beam transmitted through the sample was detected by a Si photodiode connected to the lock-in amplifier. All measurements were performed at room temperature.

3. Results and Discussion

Figure 2(a) shows the absorption spectra of the PSA1411 thin films fabricated by the different dipping times in the aqueous solution. The peak energy in the thin film of 3600 s shifts to the higher energy side, which was not observed in the previous work [22]. Unfortunately, the reason for the shift is not clear. We speculate that the shift originates from the decrease in the Coulomb force with increasing the thickness [28]. The absorbance increases with an increase in the dipping time. The value of the absorbance at 1.45 eV indicated by the dashed line in Fig. 2(a) was plotted as a function of dipping time in Fig. 2(b) using the closed circles. Note that the logarithmic scale is used for the horizontal axis. The thicknesses evaluated by the spectroscopic ellipsometry are also

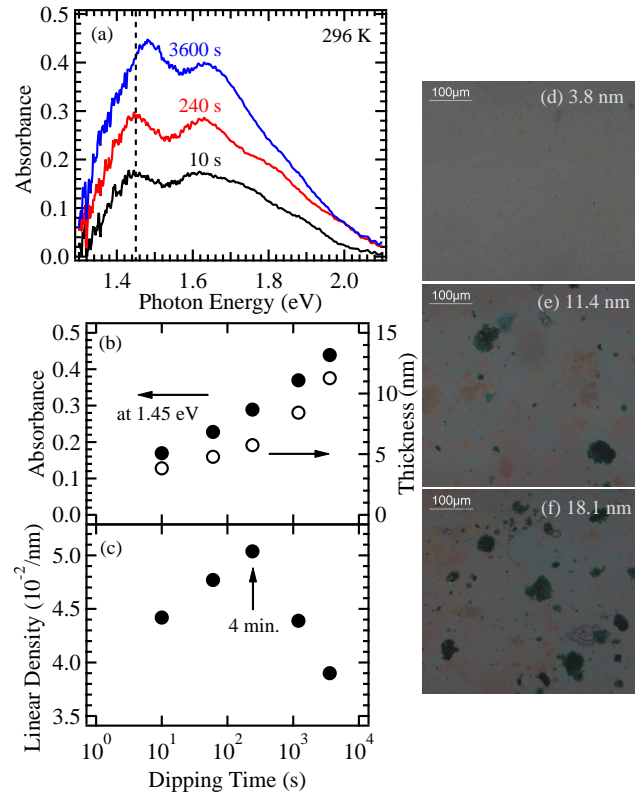


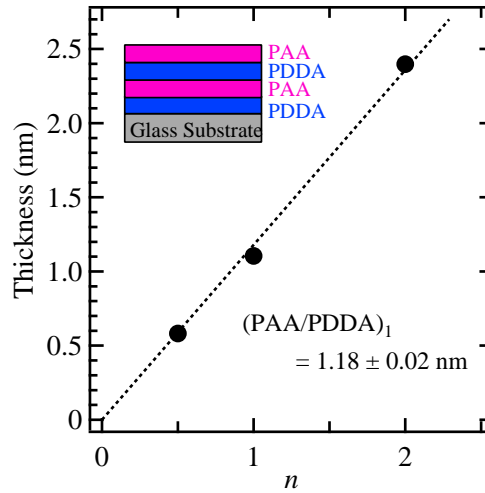
Figure 2. (a) The dependence of the absorption spectrum of the PSA1411 thin film on the dipping time. The dashed line indicates the photon energy of 1.45 eV. (b) The absorbance at 1.45 eV and the film thickness as a function of dipping time are shown by the closed and open circles, respectively. (c) The linear density of PSA1411 estimated from the coefficient obtained by dividing the absorbance by the thickness. The microscopic images for the samples with thicknesses of 3.8 (d), 11.4 (e) and 18.1 nm (f).

plotted by the open circles. The increase in the thickness almost corresponds to that in the absorbance; the increased absorbance originates from the increased film thickness rather than from larger PSA1411 in-plane density. Therefore, these results indicate that the absorbance and film thickness can be controlled by the dipping time.

However, the absorbance and film thickness do not monotonically increase with longer dipping time; this means that merely increasing the dipping time will not provide the large absorbance. Here, we focused on the relationship between the thickness and the absorbance, as shown in Table I. The relationship between the thickness and absorbance is not linear. Thus, the coefficient that corresponds to the linear density along the thickness direction was obtained by dividing the absorbance by the thickness; the coefficient was then plotted as a function of dipping time in Fig. 2(c). This result indicates that the adsorption depends on the dipping time, with the linear density coefficient reaching a maximum at 4 min. as indicated by the arrow. Furthermore, as shown in Figs. 2(d), 2(e) and 2(f), there are many molecular bundles that caused the

Table 1. The film thickness and the absorbance at 1.45 eV.

Thickness (nm)	Absorbance
3.8	0.17
4.8	0.23
5.7	0.29
8.4	0.37
11.3	0.44

**Figure 3.** The thickness of the $(\text{PAA/PDDA})_n$ bilayer (closed circles) plotted as a function of n . The dotted line indicates the least-square fitting result. The inset schematically shows the sample structure with $n = 2$.

strong scattering observed in the previous work. Therefore, to reduce the dipping time and bundle creation, we focused on the fabrication of the multilayer PSA1411 thin films.

In the multilayer structure, each PSA1411 layer is separated by the spacer layer of the $(\text{PAA/PDDA})_n$ thin film, where n is the number of the bilayer. In Fig. 3, the total thickness of the $(\text{PAA/PDDA})_n$ thin film is shown as a function of n , where $n = 0.5$ indicates a single PDDA layer. The structure of the $n = 2$ multilayer was schematically shown in the inset. The thickness clearly depends on n . Therefore, the average thickness of one PAA/PDDA bilayer was evaluated to be approximately 1.2 nm by the least-square fitting method shown by the dotted line. This result shows that the thickness of the spacer layer between the PSA1411 layers can be controlled with accuracy of 1.2 nm. Hereafter, we will refer to the thicknesses of PSA1411 and the PAA/PDDA spacer as L and R , respectively.

Figure 4(a) shows the R dependence of the absorption spectrum for two PSA1411

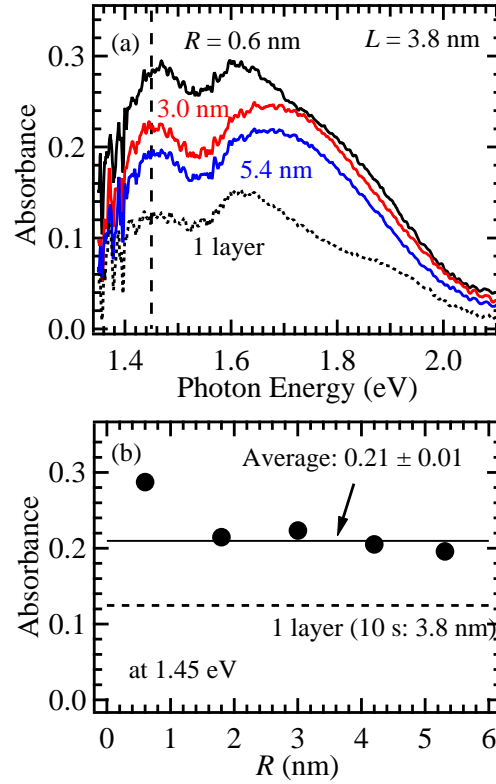


Figure 4. (a) The dependence of the absorption spectrum of PSA1411 thin film on R . The number of the PSA1411 layers is 2 and L is 3.8 nm. The dashed curve shows the absorption spectrum of the single layer thin film. The dotted line indicates the photon energy of 1.45 eV. (b) The absorbance at 1.45 eV on R . The solid and dotted lines indicate the average value of the absorbance of the samples with $R > 1$ nm and the absorbance in the single layer thin film.

layers with L of 3.8 nm. Figure 4(b) summarizes the R dependence of the absorbance at 1.45 eV shown by the dashed line in Fig. 4(a). The average value of the absorbance of the samples with $R > 1$ nm is approximately 0.21, which is almost equal to the value in the monolayer thin film fabricated by dipping for 60 s. These results show that the stacking of the PSA1411 layer provides larger absorbance for the shorter dipping time.

Figure 5(a) shows the absorption spectrum of the multilayer samples. The absorption is clearly enhanced by the increase of the number of layers. Figure 5(b) presents the dependence of the absorbance at 1.45 and 1.66 eV on the number of layers as shown by the dashed and dotted lines in Fig. 5(a), respectively. A linear increase in the absorbance clearly demonstrates the advantages of the multilayer film for the enhancement of absorbance.

A film surface without the bundles reduces the light scattering effects and is therefore a key goal for the thin film fabrication. Figure 6(a) shows a picture of the multilayer samples with $L = 3.8$ nm. It is possible to read the letters under the samples, indicating that the creation of the bundle is suppressed macroscopically. In addition,

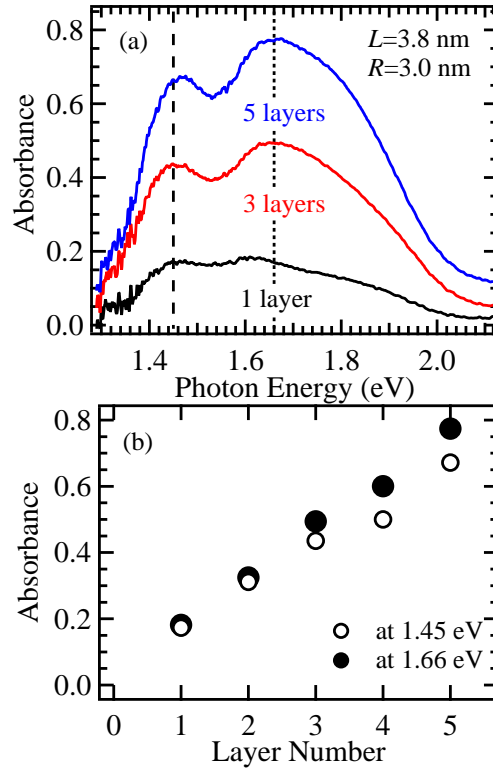


Figure 5. (a) The dependence of the absorption spectrum of the PSA1411 thin film on the number of the layers. The dashed and dotted lines indicate the photon energy of 1.45 eV and 1.66 eV, respectively. (b) The dependence of the absorbance at 1.45 eV and 1.66 eV on the number of the PSA1411 layers.

the microscopic images of the samples with three and 5 layers are shown in Figs. 6(b) and 6(c). In comparison with Figs. 2(e) and 2(f), the size and number of the bundles decrease. Hence, suppression of the light scattering can be expected.

Finally, we discuss the exciton dynamics from the viewpoint of the optical switch applications. Figure 7 shows the dependence of the pump-probe signal on the number of the PSA1411 layers with $L = 3.8$ nm and $R = 3.0$ nm. All profiles comprise two components; namely the fast component and the slow component. The result of fitting with a double exponential function is shown by the solid curves in Fig. 7. The evaluated fast relaxation time τ_1 and the slow relaxation time τ_2 are listed in Fig. 7. τ_1 and τ_2 are attributed to intramolecular and exciton relaxation, respectively. When PSA1411 is optically excited from the ground state to the lowest excited state, the intramolecular relaxation causes the rapid decay of the signal, followed by the slower exciton relaxation [28-30]. The time constants hardly change with the increase in the number of the PSA1411 layers, this clearly eliminates the possibility of exciton-exciton annihilation due to the interaction through the spacer layer in the case of $R = 3.0$ nm.

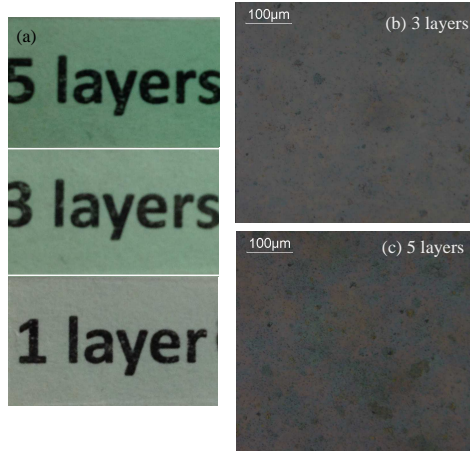


Figure 6. (a) A picture of the multilayer samples. The microscopic images for the samples with three (b) and 5 layers (c).

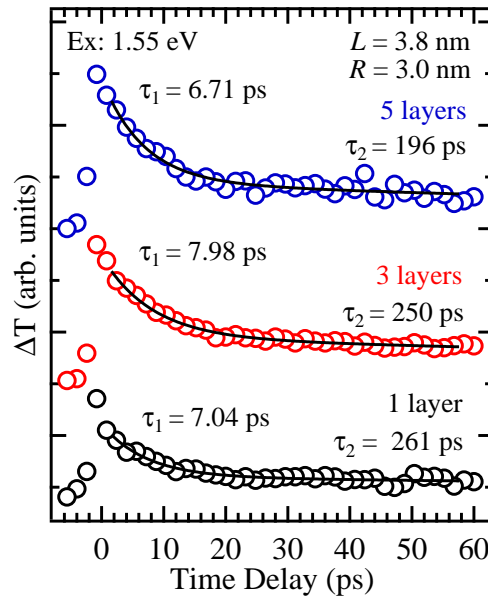


Figure 7. The dependence of the pump-probe signal on the number of the PSA1411 layers. The solid curve shows the result of fitting with a double exponential function.

4. Conclusion

We have investigated the fabrication conditions of the PSA1411 thin film by the LBL method to enable the measurement of the transient dynamics. While the absorbance and thickness of the thin film can be controlled by the dipping time, the linear density of cyanine molecules adsorbed on the substrate did not monotonically increase with longer dipping times. This precluded the achievement of large absorbance through a

simple increase of the dipping time. Conversely, by using the multilayer structure, it was possible to fabricate thin films with large absorbance in a shorter dipping time. This demonstrates the advantage of the multilayer structure fabrication. Due to the film surface without the creation of the molecule bundle, the exciton dynamics were clearly observed by the transmission-type pump-probe technique. The exciton relaxation time evaluated with double exponential function was approximately 300 ps. Therefore, these results indicate the possibility of application of the PSA1411 films in an all-optical switch operating at the repetition rate of 3 GHz. Using the energy-transfer may enhance this repetition rate.

Acknowledgments

This work was partially supported by a Grant-in-Aid for Scientific Research (Grant No. 26289088) from the Ministry of Education, Culture, Sports, Science and Technology of Japan, and the Ogasawara Foundation for the Promotion of Science and Technology.

References

- [1] Tang C W and VanSlyke S A 1987 Organic electroluminescent diodes *Appl. Phys. Lett.* **51**, 913
- [2] Fou A C, Onitsuka O, Ferreira M, Rubner M F and Hsieh B R 1996 Fabrication and properties of light emitting diodes based on selfassembled multilayers of poly(phenylene vinylene) *J. Appl. Phys.* **79**, 7051
- [3] Tao S, Zhou Y, Lee C S, Zhang X and Lee S T 2010 High-efficiency nondoped deep-blue-emitting organic electroluminescent device *Chem. Mater.* **22**, 2138
- [4] Sun N, Zhao Y, Zhao F, Chen Y, Yang D, Chen J and Ma D 2014 A white organic light-emitting diode with ultra-high color rendering index, high efficiency, and extremely low efficiency roll-off *Appl. Phys. Lett.* **105**, 013303
- [5] O'Regan B and Grätzel M 1991 A low-cost, high-efficiency solar cell based on dye sensitized colloidal TiO₂ films *Nature* **353**, 737
- [6] Zhou Q, Hou Q, Zheng L, Deng X, Yu G and Cao Y 2004 Fluorene-based low band-gap copolymers for high performance photovoltaic devices *Appl. Phys. Lett.* **84**, 1653
- [7] Wada A, Nishida J, Maitani M M, Wada Y and Yamashita Y 2014 Dye-sensitized Solar Cells Based on 1,3-Dithiol-2-ylidene Derivatives: Substituent and π -Spacer Effects on the Efficiency *Chem. Lett.* **43**, 296
- [8] Garnier F, Hajlaoui R, Yassar A and Srivastava P 1994 All-Polymer Field-Effect Transistor Realized by Printing Techniques *Science* **265**, 1684
- [9] Hepp A, Heil H, Weise W, Ahles M, Schmechel R and Seggern H 2003 Light-Emitting Field-Effect Transistor Based on a Tetracene Thin Film *Phys. Rev. Lett.* **91**, 157406
- [10] Knobloch A, Manuelli A, Bernds A and Clemens W 2004 Fully printed integrated circuits from solution processable polymers *J. Appl. Phys.* **96**, 2286
- [11] Manaka T, Liu F, Weis M and Iwamoto M 2008 Diffusion like electric-field migration in the channel of organic field-effect transistors *Phys. Rev. B* **78**, 121302
- [12] Mei J, Diao Y, Appleton A L, Fang L and Bao Z 2013 Integrated Materials Design of Organic Semiconductors for Field Effect Transistors *J. Am. Chem. Soc.* **135** 6724
- [13] Liu X, Tavares L, Osadnik A, Lausen J L, Kongsted J, Ltzen A, Rubahn H G and Kjelstrup-Hansen J 2014 Low-voltage organic phototransistors based on naphthyl end-capped oligothiophene nanofibers *Org. Electron.* **15**, 1273

- [14] Easter D C and Baronavski A P 1993 Ultrafast relaxation in the fluorescent state of the laser dye DCM *Chem. Phys. Lett.* **201**, 153
- [15] Ikeda H, Sakai T and Kawasaki K 1991 Nonlinear optical properties of cyanine dyes *Chem. Phys. Lett.* **179**, 551
- [16] Kasatani K 2002 Large electronic third-order optical nonlinearities of cyanine dyes measured by resonant femtosecond degenerate four-wave mixing *Opt. Mater.* **21**, 93
- [17] Larsen D S 2004 Stimulated emission three-pulse photo-echo peak shift: A mixed pump-probe and photon-echo technique for studying excited-state dynamics *J. Chem. Phys.* **121**, 5039
- [18] Virgili T, Lüer L, Cerullo G, Lanzani G, Stagira S, Coles D, Meijer A J H M and Lidzey D G 2010 Role of intramolecular dynamics on intermolecular coupling cyanine dye *Phys. Rev. B* **81**, 125317
- [19] Dutton G J, Jin W, Reutt-Robey J E and Robey S W 2010 Ultrafast charge-transfer processes at an oriented phthalocyanine/C₆₀ interface *Phys. Rev. B* **82**, 073407
- [20] Guarin C A, Villabona-Monsalve J P, Lopez-Arteaga R and Peon J 2013 Dynamics of the higher lying excited states of cyanine dyes. an ultrafast fluorescence study *J. Phys. Chem. B* **117**, 7352
- [21] Kojima O, Hamano S, T. Kita and Wada O 2011 Saturation of Förster resonance energy transfer between two optically nonlinear cyanine dyes of small Stokes shift energies in polymer thin films *J. Appl. Phys.* **110**, 083521
- [22] Kojima O, Fujii R, Kita T, Shim Y 2014 Control of optical properties in cyanine dye thin film fabricated by a layer-by-layer method *J. Appl. Phys.* **115**, 083503
- [23] Decher G 1997 Fuzzy nanoassemblies: toward layered polymeric multicomposites *Science* **277**, 1232
- [24] Kometani N, Nakajima H, Asami K, Yonezawa Y and Kajimoto O 2000 Luminescence properties of the mixed J-aggregate of two kinds of cyanine dyes in layer-by-layer alternate assemblies *J. Phys. Chem. B* **104**, 9630
- [25] Kim D, Okahara S, Shimura K and Nakayama M 2009 Layer-by-layer assembly of colloidal CdS and ZnS-CdS quantum dots and improvement of their photoluminescence properties *J. Phys. Chem. C* **113**, 7015
- [26] Xianda Y, Anlai W and Suqin C 1987 Water-vapor permeability of polyvinyl alcohol films *Desalination* **62**, 293
- [27] Rudnik E, 2008 *Compostable Polymer Materials* (Elsevier, Netherlands), Chap. 3.
- [28] There is a possibility that the property is different from the previous one. Though the chemical structure is same, however, the company is different.
- [29] Taylor A J, Erskine D J and Tang C L 1984 Femtosecond vibrational relaxation of large organic molecules *Chem. Phys. Lett.* **103**, 430
- [30] Weiner A M and Ippen E P 1985 Femtosecond excited state relaxation of dye molecules in solution *Chem. Phys. Lett.* **114**, 456
- [31] Haas R A and Rotter M D 1991 Theory of pulsed dye lasers including dye-molecule rotational relaxation *Phys. Rev. A* **43**, 1573